Title: Kambin's triangle and the position of the dorsal nerve root in the lumbar neural foramen

Institution paper emanated from: University of Pretoria, Pretoria, South Africa, Postal code: 0007

Authors: A. König[1], F. Joseph[2], C. Janse van Rensburg[3], J. Myburgh[1], N. Keough[1, 4]

[1]Department of Anatomy, University of Pretoria, Pretoria, Gauteng, South Africa;

[2]Department of Radiology, Steve Biko Academic Hospital, Pretoria, Gauteng, South Africa;

[3]Biostatistics Unit, South African Medical Research Council, Pretoria, Gauteng, South Africa

[4]Department of Anatomy and Cellular Biology, College of Medicine and Health Sciences (CMHS), Khalifa University, Abu Dhabi, United Arab Emirates

Abbreviated title (same as title): Kambin's triangle and the position of the dorsal nerve root in the lumbar neural foramen

*Correspondence to: Ms Anya König, Department of Anatomy, School of Medicine, Faculty of Health Sciences, Private Bag X323, Arcadia 0007, University of Pretoria, South Africa

E-Mail: anya.konig@gmail.com

PLEASE NOTE:

The abstract of this article was presented at the 47th Annual Conference of the Anatomical Society of Southern Africa in South Africa, Gauteng. The conference took place from the 7th to the 10th of

This article has been accepted for publication and undergone full peer review but has not been through the copyediting, typesetting, pagination and proofreading process which may lead to differences between this version and the Version of Record. Please cite this article as doi: 10.1002/ca.23565

April 2019. This paper has not been published, nor is it under consideration for publication elsewhere.

ABSTRACT:

Introduction: As a result of the increased utilization of neurosurgical arthroscopic techniques, investigations into population and sex specific trends of anatomical considerations have become increasingly important. This study aimed to investigate and describe aspects of the neuro-anatomical morphometry of lumbar spines in a cadaveric and MRI (Magnetic Resonance Imaging) sample.

Materials and methods: Twenty white adult (>18 years) cadavers (9 males; 11 females) were obtained under Ethical clearance. The lumbar regions were dissected and the position of the dorsal root ganglion (DRG) and dimensions of Kambin's triangle were determined. Twenty-six black adult (>18 years) MRI scans (17 males; 9 females) were obtained from an Academic Hospital and were used to determine the dimensions of the neural foramen and the DRGs within.

Results: The ganglia were mostly at the midline of the caudal pedicle. Similar to previous studies, the diagonal measurement from Kambin's triangle was the largest and the vertical measurement the shortest. Skeletal and soft-tissue measurements indicated distinct trends when moving caudo-laterally in the spine. Soft-tissue parameters from the current study were within the upper limits of those from previous studies, whereas skeletal parameters were in agreement with those reported by previous authors.

Conclusions: Results from this study suggest variation of certain parameters between studies with varying population groups, and therefore supports the need for and the importance of possible population-specific trends of anatomical parameters considered during surgical procedures.

Key Words: Kambin's triangle; lumbar spine; dorsal nerve root

TEXT:

INTRODUCTION:

The incidence of lumbar spine or lower back pathologies are rapidly increasing in our modern-day society (Hoy et al., 2010; Manchikanti, 2000). One of the most common causes of lower back pain (LBP) is herniated discs, with many cases often requiring surgical intervention (DePalma et al., 2011; Schwarzer et al., 1995). With the increase of surgical intervention in the modern age, the subsequent increase in the chances for post-operative complications is expected (Hilibrand and Robbins, 2004; Hu et al., 2014; Kumar et al., 2001; Martin et al., 2007; Park et al., 2004; Radcliff et al., 2013; Rampersaud et al., 2006). Complications relating to iatrogenic injuries of the DNRs, such as neuropathic pain or motor and sensory deficits have been reported (Antoniadis et al., 2014). Many of these complications may be reduced should the morphology of the access areas be more thoroughly reported. Researchers have been investigating morphometric properties and the variation of the human spine within individual populations in order to fill the need for population-specific anatomical parameters relevant to the safe access zones for spinal surgery(Hurday et al., 2017; Schnitzler et al., 1990; Tan et al., 2004). One such parameter used in orthopedic spinal surgery is the position of the dorsal nerve root (DNR) and ganglion (DRG) in relation to the intervertebral disc (IVD). Kambin’s triangle is an anatomical safe-zone used when approaching the IVD arthroscopically. It demarcates a safe region where the IVD can be accessed without injuring the important DNR and DRG exiting the neural foramen (Hulme et al., 2007; Matuoka and Basile Júnior, 2002; Mirkovic et al., 1995). Literature has shown population or sex specific variations with regard to the dimensions of the Kambin’s triangle (Eisenstein, 1977;

Silverstein et al., 2015; Tan et al., 2004). These variations may have substantial clinical implications with respect to arthroscopic approaches to this already small area. Understanding the extent of population- and sex-dependent variation of certain anatomical parameters specifically considered during surgical techniques, will benefit the surgical community by allowing customization of techniques that will optimize post-operative surgical outcomes (Eisenstein, 1977; Lee et al., 1995; Shaw et al., 2015; Tan et al., 2004). Knowledge of the dimensional variations should be explored and if substantial differences are noted between populations and sex groups, these variations should be communicated with surgeons to include and consider during surgical planning. Therefore, the current study investigated the neural foramen and DRG of the lumbar spine in a South African population using cadaver dissection and Magnetic Resonance Imaging (MRI) analysis.

MATERIALS AND METHODS:

Ethical considerations

This research study fell under the National Health Act (Act 61 of 2003) and the project was approved by the University of Pretoria, Faculty of Health Sciences Research Ethics Committee (320/2017). Permission was also obtained from the Hospital CEO and Head of Radiology of Steve Biko Academic Hospital to use the images.

Materials

Cadaver component

The sample comprised of twenty (n=20), white adult lumbar spines (>18 years) obtained from two local Universities (University of Pretoria and University of Witwatersrand). Specimens indicating prominent pathology such as ligamentous ossification, severe osteoporosis and scoliosis, signs of previous surgical procedures or anatomical anomalies were excluded. The total sample consisted of 9 males (78.7 ± 8.7 years) and 11 females (71 ± 16.8 years).

MRI component

The MRI sample comprised of twenty-six (n=26), black adult MRI scans (>18 years). No patient information was made known, and a unique identifier was allocated to each patient file in order to maintain anonymity. Images presenting with any pathology, trauma, or surgical interventions affecting the neural structures were excluded. The sample consisted of 17 males (37.1 ± 10.7 years) and 9 females (39.2 ± 12.3 years).

Methods

Cadaver component

Dissection

After placing the cadavers in a prone position, the superficial and deep soft-tissue was removed from the posterior skeletal elements. The spinous processes were subsequently removed with an oscillating saw, exposing the underlying dura of the spinal cord. Laminectomies were then performed on vertebral levels L1 through to L4. L5 was not included due to the difficulty accessing the vertebral body without destroying important anatomical landmarks, as well as the high variability of the L5 DNR position (Chen et al., 2013; Hogan, 1996). The pedicles were trimmed to the level of the ganglia to ensure maximum exposure of the DNR, DRG, and spinal cord.

Measurements

The DNRs were measured in relation to the pedicles, DRGs, and spinal cord using modified descriptions from two previously published studies (Matuoka and Basile Júnior, 2002; Mirkovic et al., 1995) and these measurements are demonstrated in Figure 1 (A):

1) Spinal nerve length (SNL) or diagonal border: the distance from the nerve's appearance from the dura mater to the superior border of the caudal pedicle
2) Dura-mater length (DML) or vertical border: the distance on the dura mater from the nerve's appearance to the superior border of the caudal pedicle

3) Distance from dura-mater to the nerve (DDMN) or horizontal border: the distance between the lateral edge of the dura-mater, at the superior border of the caudal pedicle to the medial edge of the spinal nerve in the transverse axis

The location of the DRG was recorded as being in one of three positions in relation to the caudal pedicle (Figure 1 (B)):

- Position A (medial foraminal): the area bordered medially by the medial edge of the caudal pedicle and laterally by the midline of the caudal pedicle
- Position B (lateral foraminal): the area bordered medially by the midline of the caudal pedicle, and laterally by the lateral edge of the caudal pedicle
- Position C (extra-foraminal): the area bordered medially by the lateral edge of the caudal pedicle

MRI component

The measurements were taken on the MRI scans using IMPAX CD viewer. These measurements are shown in Figures 2 to 4 and were defined according to those used by Hurday et al. (2017) and taken on sagittal –, axial – and coronal sections:

Sagittal section measurements (Figure 2):

- Foraminal height (FH): distance between the inferior border of the superior pedicle and the superior border of the inferior pedicle
- Foraminal diameters:

    - Superior foraminal diameter (SFD): distance between the most postero-superior edge of the IVD and the anterior surface of the facet
    - Middle foraminal diameter (MFD): distance between the most postero-middle point of the IVD and the anterior surface of the facet
    - Inferior foraminal diameter (IFD): distance between the most postero-inferior point of the IVD and the anterior surface of the facet
- Nerve root-to-pedicle distance (RP): distance between the inferior margin of the DNR and the superior margin of the caudal pedicle
- Nerve root-to-disc distance (RD): distance between the superior margin of the IVD and the inferior margin of the DNR

Distances measured above the superior margin of the IVD were considered as negative readings.

Axial section measurements (Figure 3):

- Superior margin of the IVD:
    - Foraminal AP diameter (FDS): shortest distance in the axial plane between the posterior surface of vertebral body and the anterior surface of the facet
    - Nerve root-to-disc distance (RDS): shortest distance between the DNR and the posterior surface of the IVD
    - Nerve root-to-facet distance (RFS): shortest distance between the DNR and the anterior surface of the facet
- Inferior margin of the IVD (same definitions as superior, just taken inferior to the IVD):

- Foraminal width (FDI)
- Nerve root-to-disc distance (RDI)
- Nerve root-to-facet distance (RFI)

On the coronal sections (Figure 4):

- Nerve root-to-disc measurements:
  - Medial border of the pedicle (MedD): distance from the DNR to the IVD at the medial border of the caudal pedicle
  - Middle of the pedicle (MidD): distance from the DNR to the IVD at the midline of the caudal pedicle
  - Lateral border of the pedicle (LatD): distance from the DNR to the IVD at the lateral border of the caudal pedicle
- Nerve root-to-pedicle measurements (same definitions as root-to-disc, just taken from root-to-pedicle):
  - Medial border of the pedicle (MedP)
  - Middle of the pedicle (MidP)
  - Lateral border of the pedicle (LatP)

The root-to-disc measurements that crossed inferior to the superior margin of the IVD, were considered as positive.

Statistical analysis

Statistical analyses were evaluated at a 5% level of significance and all analyses were done using STATA 14 and SPSS. For both components, descriptive statistics were generated for all measurements, and involved determining the means, standard deviations, and upper and lower limits of the 95% confidence intervals.

RESULTS:

Cadaver component

Descriptive statistics were calculated for the three sides of Kambin's triangle and are presented in Table 1. The results indicated that the diagonal border (SNL) was the longest, followed by the vertical border (DML), which was closely followed by the horizontal border (DDMN). The majority of the ganglia were found in Position B, except at L4, where the majority were found in Position C. The total ganglia found in Position A were 25, Position B were 104, and in Position C were 30.

MRI component

Sagittal slices

Neural foramen measurements

An overall increase in foraminal height was observed when moving caudally in the spine (Table 2). The largest measurement was at L5 (20.6 ± 2.4 mm), and the smallest at L1 (17.0 ± 2.2 mm). The foraminal sagittal AP diameters within each foramen decreased from superior to middle to inferior. All three AP diameters also decreased per vertebral level when moving caudally in the spine. The smallest AP diameter was found at the inferior diameter of L5 (3.8 ± 1.5 mm), and the largest at the superior diameter of L1 (8.1 ± 1.7 mm).

Nerve root measurements

The nerve root-to-pedicle – and root-to-disc distances are also shown in Table 2. The distance from the root-to-disc decreased when moving caudally with almost all levels, except when moving from L4 to L5. The distance from the root-to-pedicle increased when moving caudally with almost all levels, except when moving from L3 to L4. The DNR was superior to the IVD at all levels, with the most superior DNR at L1 (-1.3 ± 1.9 mm). The DNR was closest to the pedicle at L1 (10.4 ± 2.0 mm), and furthest at L3 (11.7 ± 2.8 mm).

Coronal slices

The descriptive statistics can be found in Table 3. The nerve root-to-pedicle distance increased when moving caudally for most medial (except from L4 to L5) and midline (except from L3 to L4) measurements. For the lateral measurements, an initial increase in distance was seen when moving from L1 to L2, followed by a decrease in distance when moving from L2 to L5. The DNR was closest to the pedicle at the lateral measurement of L4 and L5 (4.7 ± 1.8 mm and 2.3 mm, respectively) and the furthest at the medial measurement of L4 (15.9 ± 2.3 mm). The nerve root-to-disc distance increased when moving caudally for most medial (except from L4 to L5) and midline (except from L2 to L3) measurements. The lateral measurements indicated an initial decrease, followed by an increase for two levels, and a subsequent decrease from L4 to L5. The DNR was closest to the IVD at the midline measurement of L3 (-0.4 ± 2.7 mm) and the furthest at the lateral measurement of L4 (7.2 ± 1.6 mm).

Axial slices

Neural foramen measurements

The superior foraminal AP diameter in the axial plane was larger than the inferior at L1 but smaller than the inferior for L2 and L3, before becoming larger again at L4 and L5 (Table 4). The diameter at the superior border initially decreased, followed by a two-level increase, and a subsequent decrease from L4 to L5. The diameter at the inferior border increased for almost all levels except when moving from L3 to L4. The smallest foraminal AP diameter in the axial plane was at the inferior margin of the IVD at L1 (6.2 ± 0.5 mm), and the largest at the superior margin of the IVD at L4 (8.1 ± 1.7 mm).

Nerve root measurements

Table 4 shows that the DNR was situated closer to the facet for the superior measurements for all five levels and the inferior measurement of L2. The root-to-facet and root-to-disc distances showed no notable patterns of increase or decrease when moving caudally in the spine. The shortest distance from the root-to-disc was at the inferior border of the IVD at L3 (2.3 ± 0.6 mm), and the longest at the superior border of the IVD at L4 (3.2 ± 0.9 mm). The shortest root-to-facet distance was recorded at the superior border of the IVD at L2 (1.9 ± 0.7 mm), and the longest at the inferior border of the IVD at L4 (4.2 ± 1.4 mm).

DISCUSSION:

Due to the large number of spinal interventional procedures and, the growing need for less invasive techniques, possible population and sex specific anatomical structures need to be investigated and classified in order to optimise surgical outcomes. Population-specific parameters can potentially provide better insight into possible variations of anatomical structures between population groups and therefore allow surgeons to have a more personalized surgical plan for each patient. Following an intensive search of the literature, it was found that there is limited information available with regard to the differences in the neuro-anatomy of the lumbar spine. The current study therefore aimed to investigate these properties using cadaver dissection and MRI analysis.

Cadaver component

When approaching the (IVD) space arthroscopically, it is of the utmost importance to understand where vital structures lie in relation to the surgical region. This enables surgeons to avoid injury or damage to these important structures, such as the DNR and DRG, when performing arthroscopic surgery. The dissection of cadaver material provides a unique environment which enables researchers to explore the relevant anatomical parameters with precision. The use of imaging techniques also provides a view of the structures, however anatomical dissection allows a more tactile approach, and this allows the adjustment of structures which might obscure the view of those under investigation. Anatomical dissection therefore provides an unobscured view of the structures, without the concern of monitoring vital signs or having to retain irrelevant structures (in context of the specific study and study objectives) which, if removed or destroyed, could result in disabling, harming, or endangering a patient's life as would be the case in a surgical setting. Most of the ganglia were positioned in the midline (Position B) of the caudal pedicle. This seems to be in contrast to a study done by Silverstein et al. (2015), who found the ganglion to lie more laterally for levels L1 through to L5. The mentioned study included an American population (ancestry was not provided in the paper). Should a neurosurgeon with a patient from the current population base their approach on the study done by (Silverstein et al., 2015), the potential exists for an over- or under-estimated entry point, possibly resulting in a DRG injury. For Kambin's triangle measurements, the current study showed results similar to those of the Thai population for the vertical measurements and the Brazilian population for the lower level vertical measurements (L1 and L2). Also, similar results were observed for the diagonal measurements in the current study, Brazilian (Vialle et al., 2015), and Thai (Lertudomphonwanit et al., 2016) population groups. Table 5 provides an overview of measurements from the current study and compares them to those from other population groups used in previous studies

<u>MRI component</u>

MRI analysis is an ideal, non-invasive way to determine the position of the DNR and neural foramen parameters of the human lumbar spine. This is important, as a background knowledge of the location of the DNR and its relations to other structures, can aid in the surgical process and planning in order to avoid damage to this essential structure.

Neural foramen measurements

The results from the current study showed that the height of the neural foramen increased when moving caudally in the spine, a finding which could be population specific as discrepancies exist between studies. Some studies show results which align with the current study (Al-Hadidi et al., 2003; Kaneko et al., 2012; Silverstein et al., 2015), whereas others found the foraminal height to decrease when moving caudally (Hurday et al., 2017). Another supporting factor of population variation, is that the foraminal heights measured in the current study mostly lie within the upper ranges of those produced by previous authors (Al-Hadidi et al., 2003; Cinotti et al., 2002; Hurday et al., 2017; Rao et al., 2015). An inverse relationship in terms of change in measurement per level is seen with the foraminal diameters measured sagittally, where a decrease in magnitude is observed when moving caudally in the spine. As with the foraminal height, a disagreement exists between studies, with some observing a decrease in diameter caudally (Hurday et al., 2017), while others observe an increase (Torun et al., 2006). The three different diameters of each foramen (superior, middle, and inferior) differ between themselves. A clear decline in size is seen when moving caudally within the foramen itself on almost all levels, creating a typically inverted teardrop shape of the foramen, a trend which is also evident in other studies (Hurday et al., 2017; van Roy et al., 2001).

Previous authors have found that the axial foraminal measurements taken at the superior border of the IVD, are greater than those taken at the inferior border or margin of the disc (Cinotti et al., 2002; Hurday et al., 2017). This is in agreement with the current study which indicated larger axial plane foraminal AP diameter measurements superiorly. Furthermore, the current study as well as other studies (Cinotti et al., 2002; Rao et al., 2015; Torun et al., 2006) found that the axial plane foraminal AP diameter increases as one moves caudally with the spine(Hurday et al., 2017).

Nerve root measurements

Most of the nerve root-to-pedicle or disc distances measured on the sagittal scans increased when moving caudally in the spine, especially when considering the upper (L1 and L2) and lower levels (L4 and L5), and is a common feature in other morphometric studies of the lumbar DNR (Gu et al., 1999; Hasegawa et al., 1996; Hurday et al., 2017; Lien et al., 2007; Silav et al., 2016; Söyüncü et al., 2005). This means that the DNR lies above the IVD when considering the cranial levels, and gradually moves inferior to the IVD as one moves caudally in the spine.

The coronal analyses showed that for the medial measurements from the DNR to the IVD and DNR to the pedicle, the DNR was observed to be situated more superiorly in the lower lumbar levels than the higher levels. A similar trend has been recorded in other studies (Arslan et al., 2011; Gkasdaris et al., 2016; Guvencer et al., 2008; Hasegawa et al., 1996; Hurday et al., 2017; Jaskwhich et al., 1996). This relationship becomes smaller when looking at the midline of the pedicle. When moving laterally, an inverse trend is seen, in that the upper levels show larger distances between the DNR and pedicle than the lower levels. This trend was also observed by other authors (Gkasdaris et al., 2016; Hamanishi and Tanaka, 1993; Hurday et al., 2017). When looking at the axial images, the DNRs lie more anteriorly at the superior border of the IVD, and more posteriorly at the inferior border of the IVD, and is a common trend found in morphometric studies (Hurday et al., 2017; Spencer et al., 1983).

Although neurologic injury to the DRG during minimally invasive spine (MIS) surgery is a rare complication, it should be noted that the potential exists for variation between population group anatomy. MIS surgical procedures have been well researched, and approaches to various mapped safe zones have been successfully refined over time. Due to our rapidly changing lifestyles, room for further refinement and improvement of procedures will always be created. The normal DRG position in one population could easily deviate from that of another group. Therefore, surgeons should consider the possibility of population variations, investigate them, and plan their approaches accordingly – altering their standard procedures if needed. The authors intend on exploring comparative statistical analyses in order to pursue future research into more quantitative investigations of possible differences and similarities between various population groups.

The results from this study indicate that the lumbar DRG parameters vary between studies ad population groups. Therefore, this supports the need for, and importance of possible population-specific trends seen in anatomical parameters that should be considered during surgical procedures.

ACKNOWLEDGEMENTS

The authors would like to thank and acknowledge Ms Marinda Pretorius for her outstanding work in creating the illustrations used in the figures in this article.

The authors would like to thank and acknowledge the donors who provided their bodies for cadaveric materials.

The authors would also like to state that they have no conflict of interest neither financial, nor non-financial.

REFERENCES

Al-Hadidi MT, Abu-Ghaida JH, Badran DH, Al-Hadidi AM, Ramadan HN, Massad DF. 2003. Magnetic resonance imaging of normal lumbar intervertebral foraminal height. Saudi Med J 24:736-741.

Antoniadis G, Kretschmer T, Pedro MT, Konig RW, Heinen CP, Richter HP. 2014. Iatrogenic nerve injuries: prevalence, diagnosis and treatment. Dtsch Arztebl Int 111:273-279.

Arslan M, Comert A, Acar HI, Ozdemir M, Elhan A, Tekdemir I, Tubbs RS, Attar A, Ugur HC. 2011. Neurovascular structures adjacent to the lumbar intervertebral discs: an anatomical study of their morphometry and relationships. J Neurosurg Spine 14:630-638.

Chen MR, Moore TA, Cooperman DR, Lee MJ. 2013. Anatomic variability of 120 L5 spondylolytic defects. Global Spine J 3:243 - 248.

Cinotti G, De Santis P, Nofroni I, Postacchini F. 2002. Stenosis of lumbar intervertebral foramen: anatomic study on predisposing factors. Spine (Phila Pa 1976) 27:223-229.

DePalma MJ, Ketchum JM, Saullo T. 2011. What is the source of chronic low back pain and does age play a role? Pain Med 12:224-233.

Eisenstein S. 1977. The morphometry and pathological anatomy of the lumbar spine in South African Negroes and Caucasoids with specific reference to spinal stenosis. J Bone Joint Surg Br 59:173-180.

Gkasdaris G, Tripsianis G, Kotopoulos K, Kapetanakis S. 2016. Clinical anatomy and significance of the thoracic intervertebral foramen: a cadaveric study and review of the literature. J Craniovertebr Junction Spine 7:228-235.

Gu Y, Xu R, Ebraheim NA, Rezcallah AT, Yeasting RA. 1999. The quantitative study of the lateral region to the lumbar pedicle. Surg Neurol 52:353-356.

Guvencer M, Naderi S, Kiray A, Yilmaz HS, Tetik S. 2008. The relation between the lumbar vertebrae and the spinal nerves for far lateral lumbar spinal approaches. J Clin Neurosci 15:192-197.
Hamanishi C, Tanaka S. 1993. Dorsal root ganglia in the lumbosacral region observed from the axial views of MRI. Spine (Phila Pa 1986) 18:1753-1756.
Hasegawa T, Mikawa Y, Watanabe R, An HS. 1996. Morphometric analysis of the lumbosacral nerve roots and dorsal root ganglia by magnetic resonance imaging. Spine (Phila Pa 1976) 21:1005-1009.
Hilibrand AS, Robbins M. 2004. Adjacent segment degeneration and adjacent segment disease: the consequences of spinal fusion? Spine J 4:190S-194S.
Hogan Q. 1996. Size of human lower thoracic and lumbosacral nerve roots. Anesthesiology 85:37-42.
Hoy D, Brooks P, Blyth F, Buchbinder R. 2010. The epidemiology of low back pain. Best Pract Res Clin Rheumatol 24:769-781.
Hu ZJ, Fang XQ, Fan SW. 2014. Iatrogenic injury to the erector spinae during posterior lumbar spine surgery: underlying anatomical considerations, preventable root causes, and surgical tips and tricks. Eur J Orthop Surg Traumatol 24:127-135.
Hulme PA, Boyd SK, Ferguson SJ. 2007. Regional variation in vertebral bone morphology and its contribution to vertebral fracture strength. Bone 41:946-957.
Hurday Y, Xu B, Guo L, Cao Y, Wan Y, Jiang H, Liu Y, Yang Q, Ma X. 2017. Radiographic measurement for transforaminal percutaneous endoscopic approach (PELD). Eur Spine J 26:635-645.
Jaskwhich D, Zimlich R, Glaser J. 1996. Anatomy of the posterolateral disc region. Am J Orthop (Belle Mead NJ) 25:628-630.
Kaneko Y, Matsumoto M, Takaishi H, Nishiwaki Y, Momoshima S, Toyama Y. 2012. Morphometric analysis of the lumbar intervertebral foramen in patients with degenerative lumbar scoliosis by multidetector-row computed tomography. Eur Spine J 21:2594-2602.
Kumar M, Baklanov A, Chopin D. 2001. Correlation between sagittal plane changes and adjacent segment degeneration following lumbar spine fusion. Eur Spine J 10:314-319.
Lee HM, Kim NH, Kim HJ, Chung IH. 1995. Morphometric study of the lumbar spinal canal in the Korean population. Spine (Phila Pa 1976) 20:1679-1684.
Lertudomphonwanit T, Keorochana G, Kraiwattanapong C, Chanplakorn P, Leelapattana P, Wajanavisit W. 2016. Anatomic considerations of intervertebral disc perspective in lumbar posterolateral approach via Kambin's triangle: cadaveric study. Asian Spine J 10:821-827.
Lien SB, Liou NH, Wu SS. 2007. Analysis of anatomic morphometry of the pedicles and the safe zone for through-pedicle procedures in the thoracic and lumbar spine. Eur Spine J 16:1215-1222.
Manchikanti L. 2000. Epidemiology of low back pain. Pain Physician 3:167-192.
Martin BI, Mirza SK, Comstock BA, Gray DT, Kreuter W, Deyo RA. 2007. Reoperation rates following lumbar spine surgery and the influence of spinal fusion procedures. Spine (Phila Pa 1976) 32:382-387.

Matuoka CM, Basile Júnior R. 2002. Anatomical study of lumbar vertebral pedicle and adjacent neural structures. Acta Ortop Bras 10:25-34.

Mirkovic SR, Schwartz DG, Glazier KD. 1995. Anatomic considerations in lumbar posterolateral percutaneous procedures. Spine (Phila Pa 1976) 20:1965-1971.

Park P, Garton HJ, Gala VC, Hoff JT, McGillicuddy JE. 2004. Adjacent segment disease after lumbar or lumbosacral fusion: review of the literature. Spine (Phila Pa 1976) 29:1938-1944.

Radcliff KE, Kepler CK, Jakoi A, Sidhu GS, Rihn J, Vaccaro AR, Albert TJ, Hilibrand AS. 2013. Adjacent segment disease in the lumbar spine following different treatment interventions. Spine J 13:1339-1349.

Rampersaud YR, Moro ER, Neary MA, White K, Lewis SJ, Massicotte EM, Fehlings MG. 2006. Intraoperative adverse events and related postoperative complications in spine surgery: implications for enhancing patient safety founded on evidence-based protocols. Spine (Phila Pa 1976) 31:1503-1510.

Rao PJ, Maharaj MM, Phan K, Lakshan Abeygunasekara M, Mobbs RJ. 2015. Indirect foraminal decompression after anterior lumbar interbody fusion: a prospective radiographic study using a new pedicle-to-pedicle technique. Spine J 15:817-824.

Schnitzler CM, Pettifor JM, Mesquita JM, Bird MDT, Schnaid E, Smith AE. 1990. Histomorphometry of iliac creast bone in 346 normal black and white South African adults. Bone Miner 10:183-199.

Schwarzer AC, Aprill CN, Derby R, Fortin J, Kine G, Bogduk N. 1995. The prevalence and clinical features of internal disc disruption in patients with chronic low back pain. Spine (Phila Pa 1976) 20:1878-1883.

Shaw JD, Shaw DL, Cooperman DR, Eubanks JD, Li L, Kim DH. 2015. Characterization of lumbar spinous process morphology: a cadaveric study of 2,955 human lumbar vertebrae. Spine J 15:1645-1652.

Silav G, Arslan M, Cömert A, Açar HI, Kahiloğullari G, Dolgun H, Tubbs RS, Tekdemir I. 2016. Relationship of dorsal root ganglion to intervertebral foramen in lumbar region: an anatomical study and review of literature. J Neurosurg Sci 60:339-344.

Silverstein MP, Romrell LJ, Benzel EC, Thompson N, Griffith S, Lieberman IH. 2015. Lumbar dorsal root ganglia location: an anatomic and MRI assessment. Int J Spine Surg 9.

Söyüncü Y, Yldrm FB, Sekban H, Özdemir H, Akyldz F, Sindel M. 2005. Anatomic evaluation and relationship between the lumbar pedicle and adjacent neural structures: an anatomic study. J Spinal Disord Tech 18:243-246.

Spencer DL, Irwin GS, Miller JA. 1983. Anatomy and significance of fixation of the lumbosacral nerve roots in sciatica. Spine (Phila Pa 1976) 8:672-679.

Tan SH, Teo EC, Chua HC. 2004. Quantitative three-dimensional anatomy of cervical, thoracic and lumbar vertebrae of Chinese Singaporeans. Eur Spine J 13:137-146.

Torun F, Dolgun H, Tuna H, Attar A, Uz A, Erdem A. 2006. Morphometric analysis of the roots and neural foramina of the lumbar vertebrae. Surg Neurol 66:148-151.

van Roy P, Barbaix E, Clarijs JP, Mense S. 2001. Anatomical background of low back pain: variability and degeneration of the lumbar spinal canal and intervertebral disc. Schmerz 15:418-424.
Vialle E, Vialle LR, Contreras W, Jacob CJ. 2015. Anatomical study on the relationship between the dorsal root ganglion and the intervertebral disc in the lumbar spine. Rev Bras Ortop 50:450-454.

Footnotes:

[1] DML = Dura mater length; SNL = Spinal nerve length; DDMN = Distance from dura mater to nerve; SD = Standard deviation; CI = Confidence interval. Measurements are in millimeters

[2] VL = Vertebral level; SD = Standard deviation; CI = Confidence interval; FH = Foraminal height; RD = Root-to-disc distance; RP = Root-to-pedicle distance. Negative values represent measurements taken above the superior border of the IVD; SFD = Superior foraminal diameter; MFD = Middle foraminal diameter; IFD = Inferior foraminal diameter

[3] VL = Vertebral level; SD = Standard deviation; CI = Confidence interval; MedP = Medial root-to-pedicle distance; MidP = Midline root-to-pedicle distance; LatP = Lateral root-to-pedicle distance; MedD = Medial root-to-disc distance; MidD = Midline root-to-disc distance; LatD = Lateral root-to-disc distance; Negative values mean that the measurement was taken above the superior border of the IVD

[4] VL = Vertebral level; SD = Standard deviation; CI = Confidence interval; FD = Foraminal anteroposterior diameter in the axial plane; RD = Root-to-disc distance; RF = root-to-facet distance; S = Superior to the IVD; I = Inferior to the IVD

[5] Key: L = Left side; R = Right side; DML = Dura mater length (vertical border); DDMN = Distance from dura mater to nerve (horizontal border); SNL = Spinal nerve length (diagonal border); N/A =

Not applicable because the values were not recorded in the relevant study; a - (Vialle et al., 2015); b - (Lertudomphonwanit et al., 2016)

Figure Legends:

Figure 1: Image of Kambin's triangle (A), and the possible position of the DRG (B). Adapted from Matuoka and Basile Júnior (2002). Key: In A: DML = Dura-mater length (the vertical length); SNL = Spinal nerve length (the diagonal length); DDMN = Distance from dura-mater to nerve (the horizontal length). In B: A = The medial position in relation to the pedicle; B = The middle position in relation to the pedicle; C = The lateral position in relation to the pedicle

Figure 2: Graphic representation of the sagittal measurements taken. Adapted from Hurday et al. (2017). Key: In the figure on the left: RD = Distance between the dorsal nerve root and the superior border of the intervertebral disc; RP = Distance between the dorsal nerve root and the superior border of the pedicle. In the figure on the right: FH = Foraminal height; SFD = Superior foraminal diameter; MFD = Middle foraminal diameter; IFD = Inferior foraminal diameter

Figure 3: Figure indicating the measurements taken on the axial sections. Adapted from Hurday et al. (2017). Key: FD = Foraminal anteroposterior diameter in the axial plane; RD = Distance from the nerve root to the intervertebral disc; RF = Distance from the nerve root to the facet joint. Note that these measurements are the same for the levels superior and inferior to the IVD

Figure 4: Figure showing the measurements taken on the coronal scans. Adapted from Hurday et al. (2017). Key: MedP = Medial root-to-pedicle distance; MidP = Midline root-to-pedicle distance; LatP = Lateral root-to-pedicle distance; MedD = Medial root-to-disc distance; MidD = Midline root-

to-disc distance; LatD = Lateral root-to-disc distance. The dashed line indicates the superior border of the IVD

Tables

Table 1: Descriptive statistics of the borders of Kambin's triangle measured on the cadaver sample

VL	DML			SNL			DDMN		
	Mean	SD	95%CI	Mean	SD	95%CI	Mean	SD	95%CI
L1	16.0	2.1	15.3 – 16.7	21.6	2.4	20.8 – 22.4	15.4	2.3	14.7 – 16.2
L2	16.7	1.7	16.1 – 17.2	21.7	1.6	21.2 – 22.3	15.5	2.2	14.7 – 16.2
L3	16.4	1.8	15.8 – 17.0	21.0	2.1	20.3 – 21.7	15.7	2.0	15.1 – 16.4
L4	16.4	1.7	15.9 – 17.0	22.7	2.7	21.8 – 23.6	17.1	2.4	16.3 – 17.9

1

Table 2: Descriptive statistics of the foraminal height, root-to-disc –, root-to-pedicle, and foraminal diameter measurements taken on the sagittal MR images

VL	FH (mm)			RD (mm)			RP (mm)		
	Mean	SD	95% CI	Mean	SD	95% CI	Mean	SD	95% CI
L1	17.0	2.2	16.0 – 18.0	-1.3	1.9	-2.1 – -0.5	10.4	2.0	9.5 – 11.3
L2	19.2	2.4	18.1 – 20.3	-0.9	2.0	-1.7 – 0.01	11.0	2.3	9.9 – 12.0
L3	20.4	2.1	19.4 – 21.4	-0.7	2.4	-1.8 – 0.4	11.7	2.8	10.4 – 13.0
L4	20.5	2.3	19.4 – 21.6	-0.0	3.1	-1.4 – 1.4	11.1	2.8	9.8 – 12.4
L5	20.6	2.4	19.5 – 21.6	-0.6	2.7	-1.8 – 0.7	11.4	3.4	10.0 – 12.9

VL	SFD (mm)			MFD (mm)			IFD (mm)		
	Mean	SD	95% CI	Mean	SD	95% CI	Mean	SD	95% CI
L1	8.1	1.7	7.3 – 8.8	7.5	1.5	6.8 – 8.1	6.7	1.5	6.0 – 7.3
L2	7.8	1.5	7.2 – 8.5	6.9	1.7	6.2 – 7.6	6.4	1.4	5.7 – 7.0
L3	7.6	1.5	6.9 – 8.2	6.3	1.5	5.7 – 7.0	5.5	1.1	5.0 – 6.0
L4	7.0	1.5	6.4 – 7.7	5.8	1.4	5.2 – 6.4	4.8	1.0	4.3 – 5.3
L5	6.0	1.5	5.3 – 6.6	4.4	1.2	3.8 – 4.9	3.8	1.5	3.1 – 4.4

2

Table 3: Descriptive statistics of the nerve root measurements taken on coronal MR images

VL	MedP (mm)			MidP (mm)			LatP (mm)		
	Mean	SD	95% CI	Mean	SD	95% CI	Mean	SD	95% CI
L1	10.9	2.0	9.3 – 12.5	6.9	1.7	4.8 – 9.0	6.8	1.9	5.4 – 8.2
L2	13.7	2.3	11.9 – 15.4	9.0	1.4	7.9 – 10.2	7.6	2.1	5.0 – 10.2
L3	15.7	3.2	13.5 – 17.9	9.4	2.0	7.8 – 11.0	6.5	2.5	3.9 – 9.1
L4	15.9	2.3	12.8 – 19.1	8.9	1.5	6.5 – 11.4	4.7	1.8	2.5 – 6.8
L5	14.3	1.7	11.7 – 16.8	9.0	2.0	6.5 – 11.5	4.7	2.3	2.8 – 6.7
VL	**MedD (mm)**			**MidD (mm)**			**LatD (mm)**		

	Mean	SD	95% CI	Mean	SD	95% CI	Mean	SD	95% CI
L1	-5.0	1.5	-6.2 – -3.7	-0.6	3.4	-3.5 – 2.2	2.9	3.5	-0.8 – 5.8
L2	-5.7	1.4	-6.8 – -4.5	-1.5	2.5	-3.5 – 0.6	1.9	2.3	-0.02 – 3.8
L3	-7.0	2.3	-8.9 – -5.1	-0.4	2.7	-2.6 – 1.8	4.4	2.7	2.1 – 6.6
L4	-7.0	2.2	-8.9 – -5.2	0.9	2.1	-0.9 – 2.6	7.2	1.6	5.8 – 8.5
L5	-6.5	1.6	-7.8 – -5.1	-1.1	2.5	-3.2 – 1.0	5.7	2.8	3.5 – 8.1

3

Table 4: Descriptive statistics of the nerve root and foramen measurements taken on the axial MR images

VL	FDS (mm)			RDS (mm)			RFS (mm)		
	Mean	SD	95% CI	Mean	SD	95% CI	Mean	SD	95% CI
L1	7.2	0.3	6.4 – 8.0	2.6	0.3	1.9 – 3.2	2.5	0.4	1.5 – 3.4
L2	7.0	0.4	6.4 – 7.6	2.9	0.6	1.8 – 3.9	1.9	0.7	0.9 – 3.0
L3	7.6	0.7	6.9 – 8.3	2.6	0.6	2.1 – 3.2	2.1	0.7	1.5 – 2.7
L4	8.1	1.7	6.5 – 9.7	3.2	0.9	2.4 – 4.0	2.5	1.0	1.5 – 3.4
L5	8.0	1.2	7.2 – 8.9	2.9	0.7	2.4 – 3.3	2.5	1.2	1.7 – 3.4
VL	**FDI (mm)**			**RDI (mm)**			**RFI (mm)**		
	Mean	**SD**	**95% CI**	**Mean**	**SD**	**95% CI**	**Mean**	**SD**	**95% CI**

L1	6.2	0.5	4.9 – 7.5	2.9	0.6	1.5 – 4.4	3.5	0.8	1.5 – 5.5
L2	7.5	0.6	6.6 – 8.4	3.2	0.6	2.2 – 4.2	2.4	1.3	0.3 – 4.5
L3	7.8	1.4	6.5 – 9.1	2.3	0.6	1.7 – 2.8	4.1	1.5	2.7 – 5.6
L4	6.9	1.2	6.0 – 7.9	2.7	1.0	1.9 – 3.5	4.2	1.4	2.3 – 6.0
L5	7.0	0.9	6.4 – 7.7	2.7	0.6	2.3 – 3.0	4.1	1.8	2.8 – 5.4

4

Table 5: Mean and standard deviations of Kambin's triangle measurements for different population groups

Author(s)	**Population**	**DML (vertical) L**				**DML (vertical) R**			
		L1	**L2**	**L3**	**L4**	**L1**	**L2**	**L3**	**L4**
Current study	South African	16.3 ± 2.3	16.9 ± 1.7	16.6 ± 1.5	16.5 ± 1.8	15.7 ± 1.9	16.4 ± 1.7	16.3 ± 2.1	16.3 ± 1.6
a	Brazilian	N/A	N/A	14	17.52	N/A	N/A	16.55	16.4
b	Thai	17.0 ± 5.0	17.2 ± 3.8	18.7 ± 6.0	20.6 ± 3.4	15.2 ± 4.4	15.6 ± 3.8	18.4 ± 5.0	19.8 ± 5.0
		DDMN (horizontal/base) L				**DDMN (horizontal/base) R**			
		L1	**L2**	**L3**	**L4**	**L1**	**L2**	**L3**	**L4**
Current study	South African	14.8 ± 4.0	15.6 ± 2.0	15.7 ± 2.0	17.1 ± 2.2	15.7 ± 2.5	15.3 ± 2.4	15.7 ± 2.0	17.1 ± 2.7
a	Brazilian	N/A	N/A	14.25	14.55	N/A	N/A	13.75	14.17

b	Thai	11.8 ± 2.7	12.1 ± 3.0	13.6 ± 2.0	14.7 ± 2.0	13.1 ± 2.6	12.0 ± 1.8	11.3 ± 1.6	15.6 ± 2.3
		SNL (diagonal) L				**SNL (diagonal) R**			
		L1	**L2**	**L3**	**L4**	**L1**	**L2**	**L3**	**L4**
Current study	South African	21.0 ± 2.1	21.4 ± 1.8	20.4 ± 1.8	22.0 ± 2.7	22.0 ± 2.7	22.0 ± 1.4	21.4 ± 2.2	23.3 ± 2.7
a	Brazilian	N/A	N/A	18.98	23.03	N/A	N/A	21.53	21.72
b	Thai	20.4 ± 4.6	21.4 ± 4.6	23.9 ± 6.2	25.5 ± 3.0	20.1 ± 5.2	19.4 ± 4.2	21.9 ± 4.3	24.9 ± 5.6

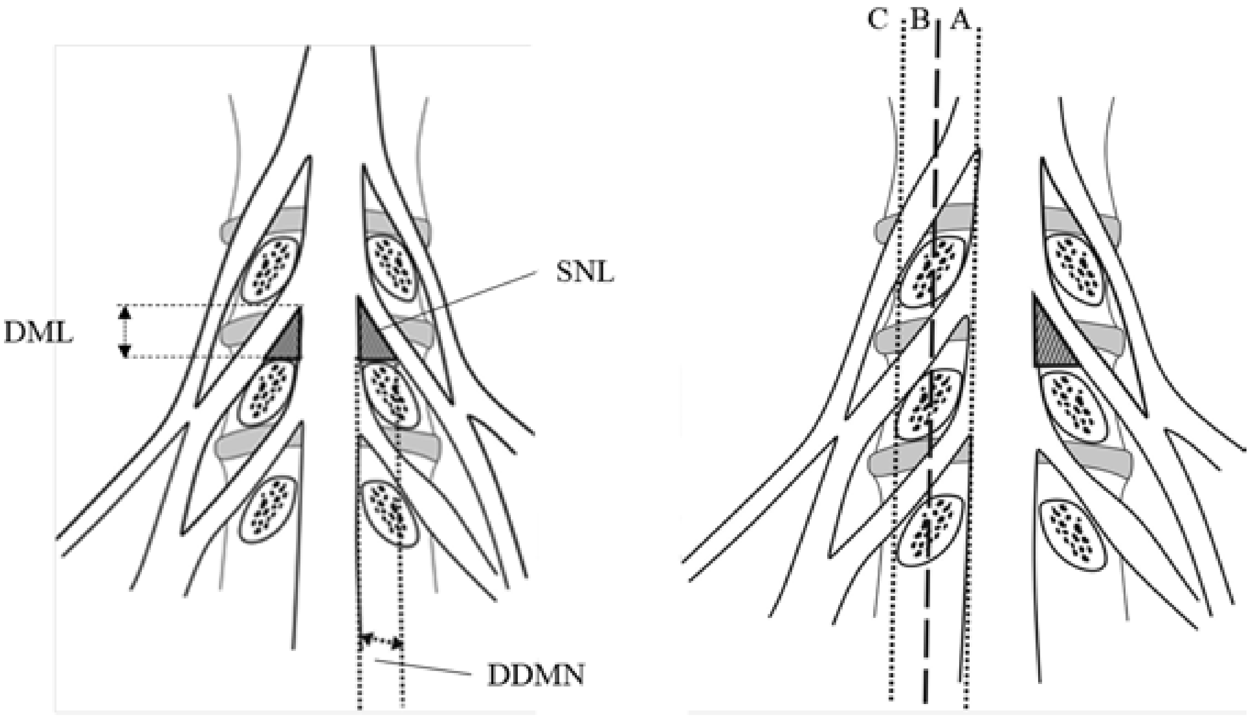

A. Kambin's triangle

B. Ganglion position

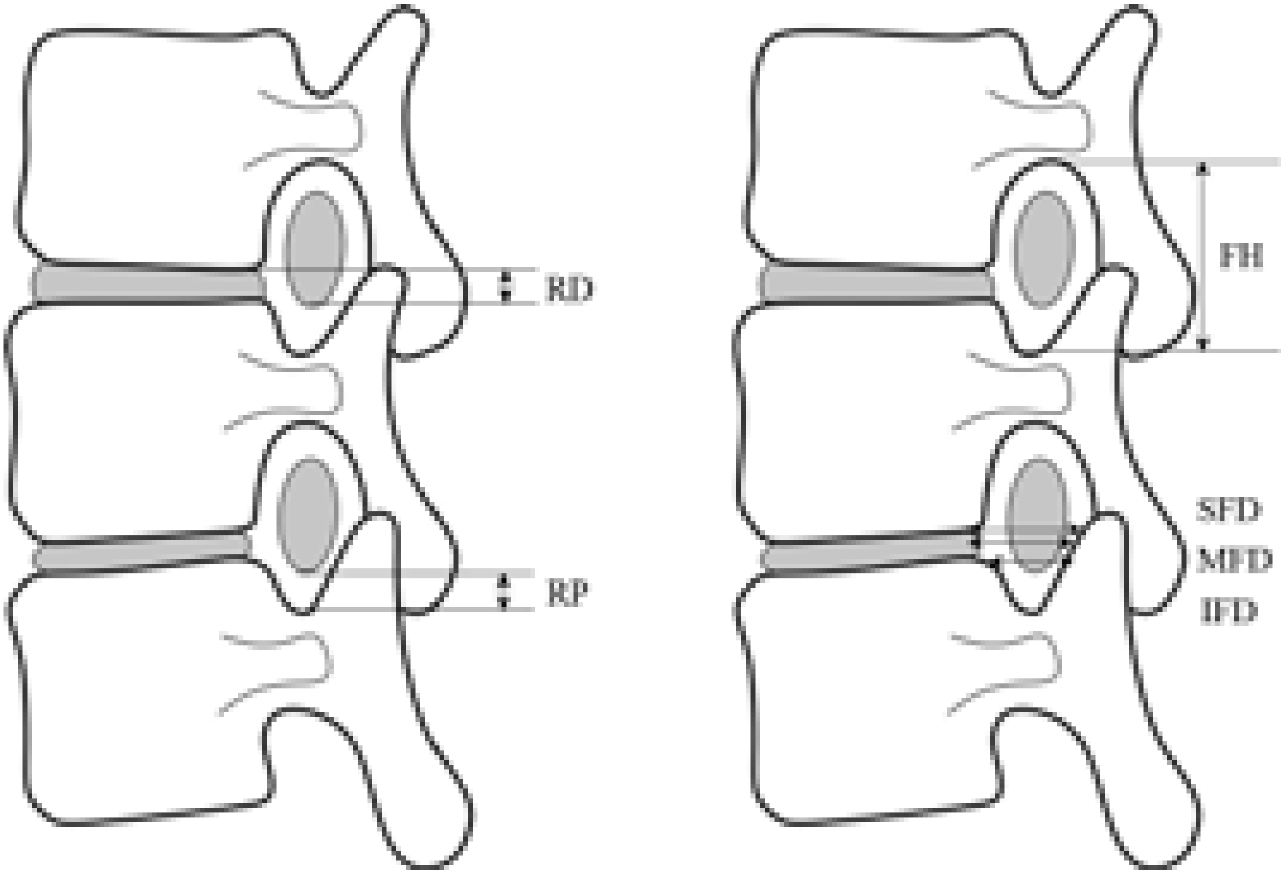
RD
RP
FH
SFD
MFD
IFD

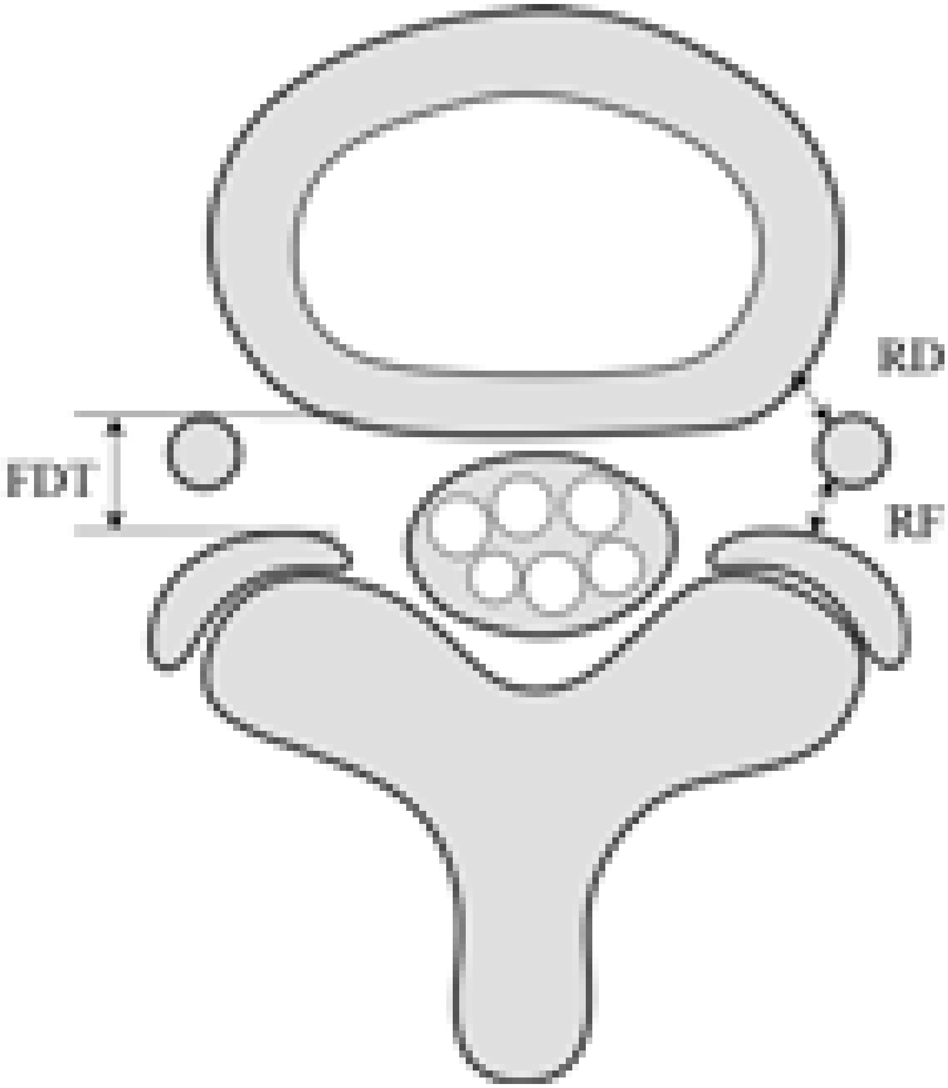
RD
FDT
RF

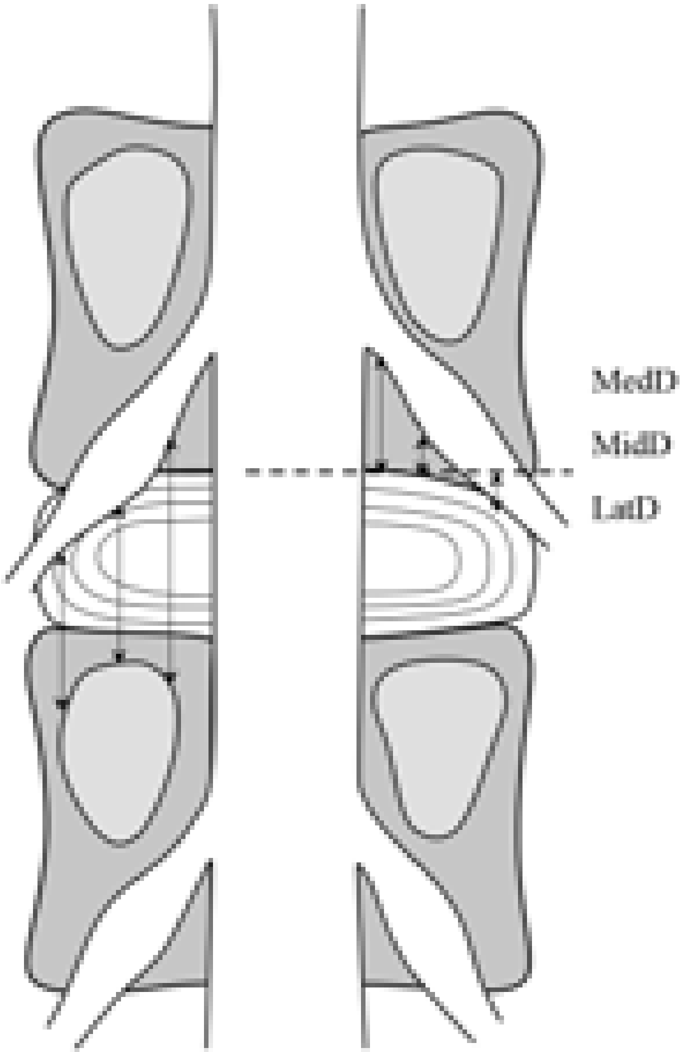
MedD
MidD
LatD
MedP
MidP
LatP